Risk Index of Regional Infection Expansion in COVID19: Moving Direction Entropy using Mobility Data and Its Application to Tokyo

Yukio Ohsawa, Yi Sun, Kaira Sekiguchi, Sae Kondo, Tomohide Maekawa, Morihito Takita, Tetsuya Tanimoto, Masahiro Kami

Submitted to: JMIR Public Health and Surveillance
on: March 02, 2024

Table of Contents

Risk Index of Regional Infection Expansion in COVID19: Moving Direction Entropy using Mobility Data and Its Application to Tokyo

Yukio Ohsawa[1] Prof Dr; Yi Sun[2]; Kaira Sekiguchi[2] PhD; Sae Kondo[3, 4] Prof Dr; Tomohide Maekawa[5] MEng; Morihito Takita[6] Dr med; Tetsuya Tanimoto[6] Dr med; Masahiro Kami[7] Prof Dr Med

[1]School of Engineering The University of Tokyo Tokyo JP
[2]School of Engineering The University of Tokyo 7-3-1 Hongo, Bunkyo-ku, Tokyo JP
[3]School of Engineering Mie University 1577 Kurimamachiya-Cho, Tsu, Mie Prefecture, 514-8507 Japan JP
[4]RCAST The University of Tokyo Tokyo JP
[5]Trust Architecture, Inc. Tokyo JP
[6]Navitas Clinic Tokyo JP
[7]Medical Governance Research Institute Tokyo JP

Corresponding Author:
Yukio Ohsawa Prof Dr
School of Engineering
The University of Tokyo
7-3-1 Hongo, Bunkyo-ku
Tokyo
JP

Abstract

Background: Policies recommending that individuals remain within their communities—including workplaces, schools, and conferences—were introduced globally to mitigate the spread of the COVID-19 pandemic. These policies meant to reduce the contacts of individuals from diverse communities: bubbling, where each should live within one's local community by reducing inter-community contacts, the Japanese policy “Stay with Your Community” (SWYC), where each sustain fewer contacts with individuals from unfamiliar communities than those in familiar ones, etc. These may be regarded as less stringent measures than Stay Home in that each can meet community members who are out of one’s family. However, these policies are inferred to be violated if individuals from various communities move to gather within close distances, which is a latent risk hard to detect in the normal conditions of society because people move complexly.

Objective: Here, we aim to create a quantifiable physical index to assess the region's compliance with the SWYC guideline, serving as a reliable alert for the potential spread of SARS-CoV-2 in the context of a case study on infectious diseases.

Methods: Moving Direction Entropy (MDE), which quantifies the diversity of moving directions of individuals in each local region, is proposed as an index to evaluate a region’s risk of violating the policy above due to the diversity of communities from which people come to meet. This index was computed for each local region using mobility data collected from smartphones.

Results: First, the MDEs for local regions showed significant invariance between different periods according to Spearman's rank correlation coefficient (>0.9). Second, MDE was found to be significantly correlated with the rate of infection cases of COVID-19 over local populations in the 53 inland regions of Tokyo: 0.76 in average during the periods of expansion. The density of restaurants had a similar correlation with COVID-19. The densities of schools and listed companies were correlated with Influenza and STDs, respectively. Third, the spread of COVID-19 infection was accelerated in regions with high-rank MDEs than in those with high-rank densities of restaurants during and after the period governmental declarations of emergency ($p < .001$). This finding is explained as due to policymakers’ overlooking of MDE. Fourth, MDEs tended to be high and increased during the COVID-19 period in regions where influx or daytime movements were active.

Conclusions: We propose monitoring the regional values of MDE to reduce the risk of infection spread. To aid this monitoring, we show a method to create a heat map of the MDE values, thereby drawing public attention to the hazards of behaviors that facilitate contact between communities during a highly infectious disease pandemic. Clinical Trial: We are not registered in a WHO-accredited trial registry. because this study used mobility data from smartphones and other available data without trials.

(JMIR Preprints 02/03/2024:57742)

DOI: https://doi.org/10.2196/preprints.57742

Preprint Settings

1) Would you like to publish your submitted manuscript as preprint?

Please make my preprint PDF available to anyone at any time (recommended).

Please make my preprint PDF available only to logged-in users; I understand that my title and abstract will remain visible to all users.

Only make the preprint title and abstract visible.

✓ **No, I do not wish to publish my submitted manuscript as a preprint.**

2) If accepted for publication in a JMIR journal, would you like the PDF to be visible to the public?

✓ **Yes, please make my accepted manuscript PDF available to anyone at any time (Recommended).**

Yes, but please make my accepted manuscript PDF available only to logged-in users; I understand that the title and abstract will remain v

Yes, but only make the title and abstract visible (see Important note, above). I understand that if I later pay to participate in <a href="http

Original Manuscript

Original Paper

Authors and Affiliations:
Yukio Ohsawa, Professor, PhD. *1
Yi Sun, Mr. *1
Kaira Sekiguchi, Dr. *1
Sae Kondo, Associate Professor, PhD. *2,*3
Tomohide Maekawa, Mr. *4
Morihito Takita, MD. *5
Tetsuya Tanimoto, MD. *5
Masahiro Kami, MD. Professor, PhD. *6

*1: Department of Systems Innovation, School of Engineering, The University of Tokyo
*2: Research Center for Advanced Science and Technology, The University of Tokyo
*3: Department of Architecture, School of Eng. Mie University
*4: Trust Architecture, Inc., Tokyo
*5: Navitas Clinic, Tokyo
*6: Medical Governance Research Institute, Tokyo

Authors Contribution:
YO: Conceptualization, data collection, data analysis, writing
YS: Data collection, data analysis
KS: Data collection, data interpretation
SK: Conceptualization, data collection, data interpretation
TM: Data collection, data interpretation
MT, TT, and MK: data interpretation and organizing the paper

Trial Registration: This study was not registered in a clinical trial registry because it used mobility data from smartphones and other available data, without trials.

Risk Index of Regional Infection Expansion in COVID19*:* Moving Direction Entropy using Mobility Data and Its Application to Tokyo

Corresponding author: Yukio Ohsawa, ohsawa@sys.t.u-tokyo.ac.jp

Abstract

Background: Policies such as Staying Home, bubbling, and Staying with Your Community, recommending that individuals reduce contact with diverse communities, including families and schools, have been introduced to mitigate the spread of the COVID-19 pandemic. However, these policies are violated if individuals from various communities gather - a latent risk in the real society where people move among various unreported communities.

Objective: We aimed to create a physical index to assess the possibility of contact between individuals from diverse communities, which serves as an indicator of the potential risk of SARS-CoV-2 spread if taken into account combined with existing indices.

Methods: Moving Direction Entropy (MDE), which quantifies the diversity of moving directions of individuals in each local region, is here proposed as an index to evaluate a region's risk of contacts of individuals from diverse communities. MDE was computed for each inland municipality in Tokyo using mobility data collected from smartphones from before to during the COVID-19 pandemic. To validate the hypothesis that the impact of inter-community contact on infection expansion becomes larger for a virus with larger infectivity, we compared the correlations of the expansion of infectious diseases with indices including MDE and the densities of supermarkets, restaurants, etc. In addition, we analyzed the temporal changes in MDE in municipalities.

Results: First, the MDEs for local regions showed significant invariance between different periods according to Spearman's rank correlation coefficient (>0.9). Second, the MDE was found to correlate with the rate of infection cases of COVID-19 over local populations in the 53 inland regions: 0.76 in average during the periods of expansion. The density of restaurants had a similar correlation with COVID-19. The correlation with MDE was higher for COVID-19 than for influenza, which was higher than for sexually transmitted diseases, that is, in the order of infectivity, which supports the hypothesis in Methods. Third, the spread of COVID-19 was accelerated in regions with high-rank MDEs compared to those with high-rank restaurant densities during and after the period of governmental declarations of emergency ($p < .001$). Fourth, the MDEs tended to be high and increased during the pandemic period in regions where influx or daytime movement was active. A possible explanation for the third and fourth findings is that policymakers and living people have been overlooking MDE.

Conclusions: We propose monitoring the regional values of MDE to reduce the risk of infection spread. To aid in this monitoring, we present a method to create a heat map of MDE values, thereby drawing public attention to behaviors that facilitate contact between communities during a highly infectious disease pandemic.

Keywords: suppressing the spread of infection; index for risk assessment; local regions; diversity of mobility; mobility data; moving direction entropy (MDE); social network model; COVID-19; Influenza; sexually transmitted diseases

Introduction

During the COVID-19 pandemic, policies, including stay-at-home and social distancing, have been introduced worldwide [1] as measures for terminating synchronized mobility. Although these measures delay or suppress COVID-19 infections during their application period [2,3], several adverse effects have been reported: infections of specific viruses in patients staying home or hospitals have increased [4, 5]; mental stress, economic inactivity, domestic violence, and variations in the types of crimes have been reported [6-10] especially in urban regions with high population density, which alone cannot always explain the phenomenon of infection spread [11].

Thus, other measures have been developed, such as the Stay with Your Community (SWYC) [12], which was introduced in Japan in December 2020 [13,14] as a measure to suppress infection expansion. SWYC refers to sustaining fewer contacts with individuals from unfamiliar communities than with those from familiar communities, where community refers to a group of people whose members frequently come into an infectious connection in daily life. The spread of infection is estimated to be significantly magnified if individuals violate the SWYC. Other governmental measures studied in [3,4.15] can also be regarded as approaches to sustaining fewer contacts with unfamiliar individuals. These can be regarded as solutions to suppress the spread of infection via inter-community contact resulting from globalization, urbanization, and mobility [16-18], and as a mild strategy in the sense that it is less stringent than Stay Home because each individual can meet community members, who may be classmates or colleagues in the workplace, and even than the "bubbling" strategy where each should live within one's local community called a bubble by cutting off inter-community contacts [15]. Constraint to sustain fewer contacts with individuals from unfamiliar communities, which we refer to as constraint on intercommunity contacts hereafter. is inferred to be violated if individuals from various communities (offices, schools, conferences, etc.) gather in a place narrow enough for them to contact each other within a sufficiently close distance of the infection. However, an index to quantify the extent of non-adherence to the constraint on intercommunity contact, which can be measured physically, has been missed.

In this study, we developed a new index that can be physically quantified and used to assess the risk of infection spreading in each local region. By a "local region, " we refer to a defined range of space, such as a municipality (a city, ward, or village; excluding islands here), as a part of a prefecture or a meshed area of a certain width (e.g., 1 km square). In the cases of necessity, we clarify the corresponding geographical area in the remainder. The index we propose integrates mobility and inter-community connectivity, which are key factors contributing to the spread of infection in each local region. In terms of mobility, the correlation between human movement and infections has been analyzed [30,31], and viruses transmitted by mosquitoes have been found to be partially driven by human mobility [32]. Specifically, the radius of gyration has been used to measure activities that affect the spread of infection in urban areas [33,34]. On the other hand, it has been discovered that a local region embracing the diversity of mobility patterns can show various responses to changes in an environment where various communities interact [35-37]. Controlling such complex interactions through interventions focused on popular venues, where participants gather from various communities, may reduce both the peak infection rate and the total infected population, while retaining high social activity levels [38].

Partial differential equations have been used to predict the spread of infection via inter- and intra-regional interaction [39]. The Silent Index for five industrial domains in a country has been shown to correlate with COVID-19 infection cases by a lag of weeks [40] but is not applicable to risk estimation for a finer mesh of 100m or 1 km square or by finer temporal resolution, which is desired for proposing ways to live in each local region [14]. In the present study, we highlight the diversity of people’s moving directions, to which moving individuals may not pay attention, as a risk factor for local regions breaching the constraint on intercommunity contact due to increased opportunities for individuals from different communities to meet in a single location.

In this study, we show the correlation between a new index, the Moving Direction Entropy (MDE), as shown in the **Methods** section, which represents the diversity of the moving directions of individuals in each local region and the spread of infection. We assumed that the direction of an individual's movement reflects one’s interest in moving to or from the community. Based on this assumption, and using a dataset on the movements of individuals, we expected the MDE to represent the extent to which the constraint on intercommunity contact would be violated. Thus, we computed the correlation between the rate of infection in the population and MDE in a local region to evaluate

the utility of MDE as a measure of the risk of infection expansion. The correlations between MDE and other infectious diseases, such as influenza and STDs, were also evaluated. We found that MDE is strongly correlated with the spread of COVID-19 and evidence supporting Hypothesis A. Furthermore, we computed the temporal variation in MDE values for local regions in Tokyo to clarify the changes in the non-adherent activities of individuals in urban settings. Finally, we propose applications of MDE as a new risk measure for suppressing infection expansion and the use of an urban risk map.

Methods

Hypothesis: Virus infectivity and impacts of intercommunity contacts

To consider situations that violate the constraint on intercommunity contact, we set Hypothesis A below regarding the tendencies of different infectious diseases during the expansion of infection:

Hypothesis A: If the infectivity of a virus, defined as the number of others that an infective individual can infect, is larger, the impact of intercommunity contact on infection expansion becomes larger.

The intuitive meaning of Hypothesis A is illustrated in Figure 1, using a social network model. To consider the structural features of contacts, the spread of infection has been modeled using social networks [19-25]. To understand the influence of the above constraint violation on the spread of infection, it is desirable that contacts among individuals be controlled by setting node degrees for strategic manipulation of social networks, as in [23]. For example. The SWYC was discovered in [12] using scale-free networks, among other models, modified by reflecting spatiotemporal constraints in real society on the degrees of nodes in the network. Sexually transmitted diseases (STDs) have been analyzed using social network models [24] and were also modeled using scale-free networks [25].

In Fig. 1, the edges represent infectious contacts among individuals and the communities are represented by thick edges. Multiple communities are densely interconnected via thin edges in Fig.1**A** and **C** forming a large connected subgraph that includes inter-community contacts represented by thin edges, that is, less frequent than within each community represented by thick edges. Fig.1**B** and **D** are composed of smaller connected subgraphs than those in Fig.1**A** and **C**. Hypothesis A states that infection spreads widely across communities if inter-community infectious bridges, shown by the thin edges, are dense owing to the strong infectivity of the virus via individuals attending inter-community meetings in real spaces (orange shadows in Fig.1), as shown in Fig.1**C**. That is, the widened inter-community meeting places in the orange shadows, as in **C** and **D,** mediate infections only if inter-community bridges are dense, as in **C** where infectious connections exist in the meeting places.

Fig. 1**A** and **C** correspond to highly infectious diseases, such as COVID-19, or infections in densely populated areas, such as restaurants, in urban regions. Fig.1**B** and **D** show a disease with low infectivity, such as STDs, that normally transmit only via intimate contact or exceptional hubs, such as prostitutes. Therefore, the node degrees here are assumed to be lower, corresponding to low infectivity [26]. A moderately infective species, such as influenza, whose infectivity based on the basic reproduction number is lower than that of COVID-19 [27-29] or COVID-19 in less populated areas, is positioned as an inter-community bridge of intermediate strength between Fig. 1**A**/**C** and Fig.1**B**/**D**. Based on the literature, we assumed that influenza was less infectious than COVID-19, and influenza, including H7N9, H5N1, H1N1, etc., was compared with COVID-19 before February 2021[12]. Xue et al. compared Omicron and influenza (seasonal and 2009 H1N1) on transmission rate and effective reproduction number (*Re*) [28]. Daemi et al. used the basic production number to compare H1N1 and COVID-19 before the appearance of Omicron [29].

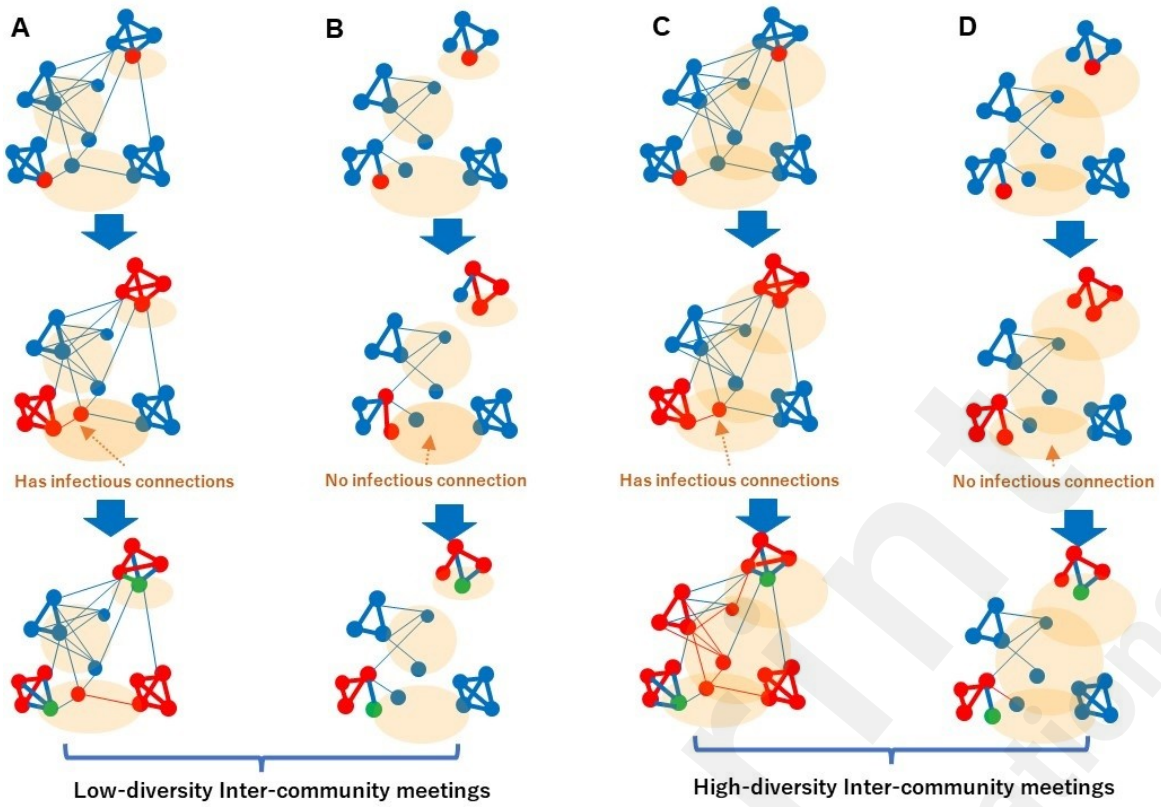

Figure 1. Viral infections spread across two types of networks. **A** and **C**: Strong inter-community bridges (for example, COVID-19), **B** and **D**: weak inter-community bridges (e.g. STDs). Influenza is positioned as of inter-community bridges of intermediate strength. Meeting places are represented by the orange shadows, as in **C** and **D.**

Moving Direction Entropy

To date, data on human mobility have been used to analyze the spread of COVID-19. In [41], the effect of social distancing was evaluated. However, it is difficult to obtain accurate results for the medium-term COVID-19 pandemic [42] because of the nonlinear relationship between the number of COVID-19 cases and human mobility. In this study, we focused on the diversity of people's moving directions using an entropy-based index, among other physical features such as the distance between individuals. To consider the diversity of the moving directions of individuals in each local region, we developed the MDE below: This statistical entropic feature is obtained by aggregating movements to generate inferences about intercommunity contacts on a regional scale. The limitations of this approach will be discussed later in the Limitations section in the Discussion.

We define the MDE in region r at time t as in Eq.(1), where θ denotes the anticlockwise angle of the moving direction and 0 [rad] for the north. θ is discretized by segmenting 2π into 100 segments (π /50 each). p_θ (r, t) is the probability that an individual moves in the [θ, θ +π/50] direction in region r at time t.

$$H_{MDE}(r,t) = -\sum_{i=1}^{100} p_{\theta=i\pi/50}(r,t)\log p_\theta(r,t) \qquad (1)$$

This definition diverts information entropy, established in information science, to consider the diversity of the collected information. to model the behavior of individuals. Thus far, the entropy of individual trajectories has been used to study the relevance of mobility diversity to social behavior,

socioeconomic indicators, and spatial attractiveness [43-45]. In the traditional mathematics of information entropy, the error in the sensors does not affect the ordinal results of the MDE for local regions for the following reason. That is, the value $H_{ERR}(r, t)$, an error function of a normal distribution with a standard deviation σ representing the sensing error of the moving direction, is a constant H_{ERR} for each (r, t) as long as σ is a constant. The value of $H_{\mathrm{MDE}}(r, t)$ obtained from the sensor data is the sum of $H_{ERR}(r, t)$ and the true value of $H_{\mathrm{MDE}}(r, t)$ because $H_{\mathrm{MDE}}(r, t)$ is the convolution of $H_{\mathrm{MDE}}(r, t)$ and $H_{ERR}(r, t)$. Thus, we do not include error bars in the analysis and discussion because we evaluate the ranking of MDEs values, including $H_{\mathrm{ERR}}(r, t)$, which is constant.

We applied Eq.(1) to the Used Dataset 1, setting r to each municipality for the experiments in Results, and meshes (100m or 1 km square) for creating the maps in the Conclusions. We then compared the results with the infection cases in the Used Dataset 2 by referring to the populations in the Used Datasets 3 and 4.

In summary of the Methods section, (1) we hypothesized that the effect of intercommunity contacts is expected to be more significant if the infectivity of the target virus is high (as of COVID-19); thus, the risk of intercommunity contacts can be estimated by MDE, so that (2) we use MDE as an index for estimating the pandemic risk of COVID-19, which is of high infectivity based on the expectation from the hypothesis in (1).

Data sources

The collected data are summarized as follows: Further information is provided in the **Multimedia Appendix 1.**

Used Dataset 1: Point data on human movements

The first dataset used was point data on human movements in Tokyo provided by Agoop Inc. Simply put, the location and velocity were sensed using a GPS sensor embedded in the smartphone.

Used Dataset 2: The number of infection cases

Data on the number of infection cases were collected for comparison with the MDE values. (a) COVID-19, (b) other infectious diseases.

Used Dataset 3: Population of each local region

To validate Hypothesis A used the dataset for the population in Tokyo: (a) permanent habitats, (b) daytime populations, and (c) influx movements, provided as open data. These regions include 53 land segments, excluding the islands of Tokyo.

Used Dataset 4

Number of institutions (restaurants, supermarkets, etc.) in each region of Tokyo.

Results

As shown in Fig.2, positive correlations were found between MDE and the rate of infection cases (number per 10^4 people) for COVID-19 in each of the 53 local regions and all municipalities, excluding islands in Tokyo Prefecture. First, we confirm that the MDEs for all local regions are substantially invariant according to Spearman's rank correlation coefficient (> 0.9) between the MDEs of different periods, as shown in Table 1 (corresponding to the worksheet “Table 1 Correlation of MDEs” in Generated Dataset 1 in Multimedia Appendix 1). We obtained the MDEs for the periods of missing data (rows and columns with “*” in Table 1) using linear completion from adjacent periods. When linear completion was impossible due to missing mobility data within three months of the target infection cases (April 2020), we used the MDE of April 2021,

considering the similarity of human behaviors in the same season.

As a result, as shown in Table 2 (corresponding to the worksheet “Table 2 Indices and cases” in Generated Dataset 1 in Multimedia Appendix 1), the value of Spearman's rank correlation between MDE and the infection cases of COVID-19 in municipalities is over 0.6 for all periods, 0.76 with an average, of COVID-19 expansion. The correlation values were relatively low in December 2020 and October 2021, during which the correlation also decreased for other indices showing the densities (i.e., the number of restaurants, supermarkets, etc. per km^2) obtained from the Used Dataset 4. Note that the values of *X* and *Y* in Fig. 2 are divisions by area width and population, respectively, which means that there is no effect mediated by the region size. As shown in Table 2, the correlation between MDE and the rate of infection was smaller for influenza than for COVID-19, and tended to be even smaller for STDs.

Furthermore, the following tendencies were observed.

(i) The MDE and number of restaurants were most strongly correlated with the rate of COVID-19 infection during the tested periods (orange vertical bars in Fig.S1 in Multimedia Appendix 1).

(ii) Influenza is correlated with MDE less strongly than COVID-19 but is more strongly correlated with the densities of (elementary, junior, and high) schools.

(iii) The density of listed companies had higher correlations with STDs than with other indices.

Regarding (i), after the periods of governmental declarations of emergency, rapid upward trends were found in cities with high-rank MDEs and low-rank restaurant densities, as shown in Fig.3 (corresponding to Generated Dataset 2 in Multimedia Appendix 1). As shown in columns BU and BV in the worksheet “Table 2 Indices and cases,” of Generated Dataset 1 in Multimedia Appendix 1, local regions that did not have a high-rank density of restaurants (ranked lower than the 20^{th}) found a significantly larger expansion if they were relatively highly ranked on MDE (within the 30^{th} highest) than those with higher than the 20^{th} density of restaurants ($p < .001$).

In Fig. 4**A** from Generated Dataset 3 in Multimedia Appendix 1, the upper-right (lower-left) cluster includes local regions with larger (smaller) MDE and larger (smaller) numbers of infected cases. The locations of these regions are shown on the map of Tokyo in Fig.4**B**. In Fig. 5, the regions are classified based on their population densities of (**a**) permanent habitats, (**b**) daytime, and (**c**) influx in the Used Dataset 3.

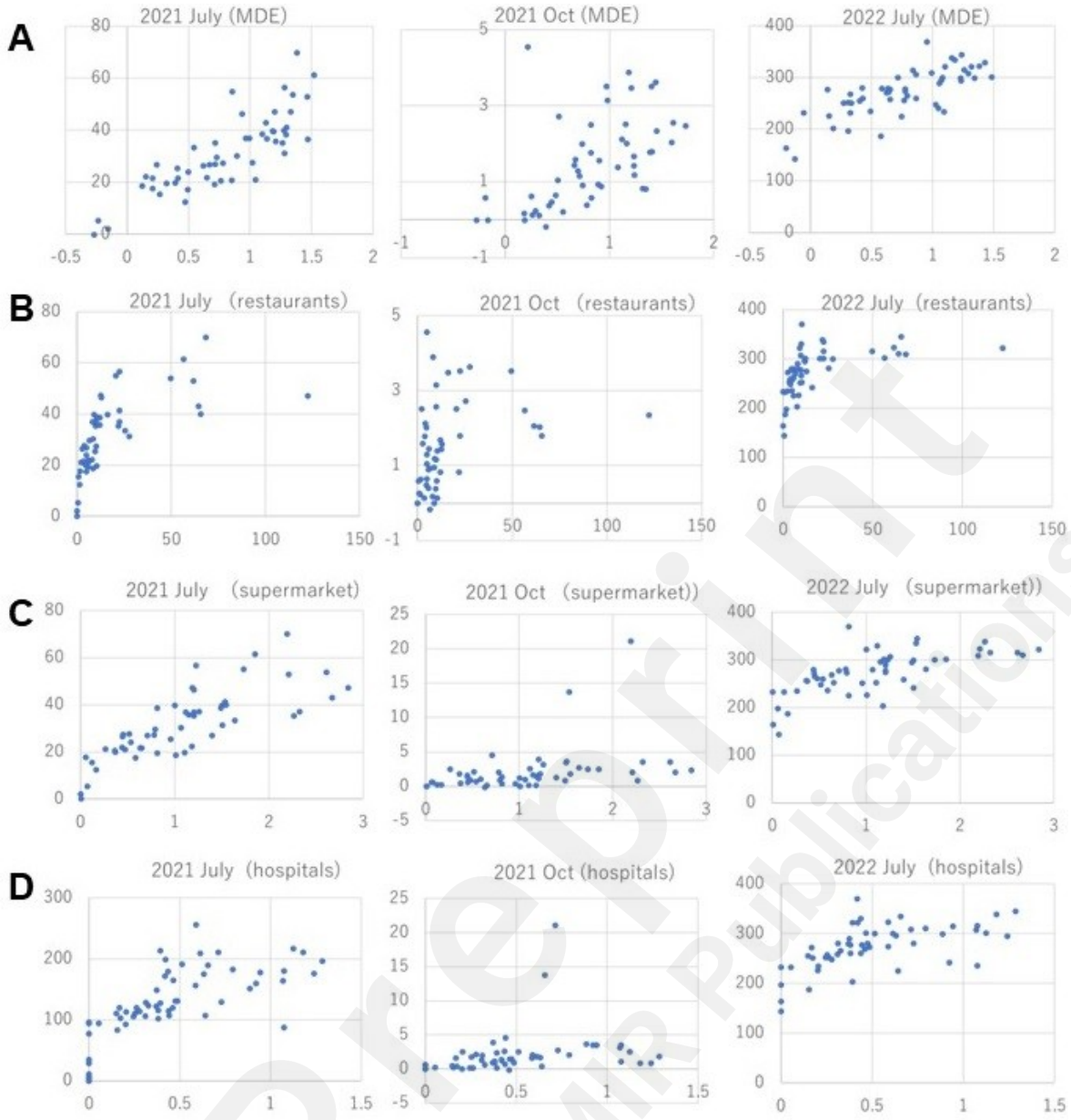

Figure 2. Correlation between X as **A:** MDE, and the densities (numbers per km^2) of **B:** restaurants, **C:** supermarkets, and **D:** hospitals, versus the rates (cases per 10^4 habitats) of infection cases (Y: COVID-19): The dots represent the values of (X, Y) for the 53 municipalities in Tokyo excluding islands. Note that both values do not reflect the population but are the rates obtained by dividing the number by the width or population of each city. MDE is converted here for visualization to $-\log\left(4.6-H_{MDE}\right)$.

Table 1. The invariance of MDE values in local regions, quantified by the Spearman's rank correlation for the 53 local regions in Tokyo, between different periods corresponding to Table 2. The dates show the periods the MDE values were computed. The rows and columns with "*" here shows the MDEs for periods of missing data using linear completion from adjacent periods.

	(1)	(2*)	(3)	(4*)	(5)	(6)	(7*)	(8)	(9)
(1) Dec 5-11, 2019	1.0	.96	.96	.93	.91	.91	.91	.91	.92
(2) Oct 10, 2020 (*)	.96	1.0	1.0	.96	.94	.93	.92	.92	.92
(3) Dec 3-9, 2020	.96	1.0	1.0	.97	.94	.93	.92	.91	.91
(4) Apr 1, 2021 (*)	.93	.96	.97	1.0	.99	.99	.98	.98	.98
(5) Jul 26-8/9, 2021	.91	.94	.94	.99	1. 0	.99	.99	.99	.99
(6) Oct 18-31, 2021	.91	.93	.93	.99	.99	1.0	1.0	1.0	.99
(7) Apr 1, 2022 (*)	.91	.92	.92	.99	.99	1.0	1.0	1.0	1.0
(8) Jul 25-Aug 8, 2022	.91	.92	.91	.99	.99	1.0	1.0	1.0	1.0
(9) Oct 17–30, 2022	.92	.92	.91	.98	.99	.99	.99	1.0	1.0

Table 2. Correlation of the rate of infection cases (COVID-19, STDs, and influenza) and explanatory indices (MDE and the densities of institutes in local regions) quantified by the Spearman's rank correlation for the 53 local regions in Tokyo: The MDE values were computed on the Used Dataset 1 for each period in a blue square in Fig.S1, and the rates of cases were obtained from the Used Dataset 2 for each period of two weeks - in an orange-colored bar in Fig.S1 for COVID-19. The *P* values show the significance of the superiority of MDE to other indices. Note: the dates are the beginning of two weeks the numbers of infection cases were counted.

	Rates of infection cases: COVID-19 of three years

		2020				2021			2022			Aver-age	t-test
		Before 5-Apr	26-Jul	17-Oct	3-Dec	1-Apr	26-Jul	18-Oct	25-Jan	1-Apr	25-Jul		
Indices													
MDE		.77	.83	.73	.62	.84	.85	.67	.87	.71	.75	.77	
The density (/km^2) of													
	Restaurants	.74	.86	.77	.65	.82	.85	.55	.83	.76	.78	.76	p =.37
	Super-markets	.74	.81	.77	.66	.75	.83	.58	.8	.77	.73	.74	p =.11
	elementary schools	.65	.83	.69	.54	.74	.8	.6	.76	.73	.74	.71	p =.002
	High schools	.62	.78	.72	.57	.7	.79	.55	.72	.67	.67	.68	p <.001
	junior high schools	.66	.81	.72	.56	.73	.8	.63	.73	.73	.72	.71	p =.004
	train stations	.67	.83	.74	.63	.79	.79	.56	.82	.71	.77	.73	p =.02
	Hospitals	.56	.7	.65	.56	.68	.69	.54	.71	.57	.66	.63	p <.001
	listed companies	.72	.82	.73	.6	.78	.81	.59	.79	.74	.77	.74	p =.022
	population	.7	.86	.71	.55	.76	.84	.65	.78	.71	.75	.73	p =.011

		STDs, 3-17 Dec 2019				Influenza
		Gonorrhea	Genital herpes	Chlamydia	Condyloma acuminatum	
Indices						
MDE		.48	-.06	.56	-.18	.45
The density (/km^2) of						
	restaurants	.53	-.06	.6	-.15	.38
	supermarkets	.49	-.08	.57	-.17	.44
	elementary schools	.43	-.12	.52	-.22	.43
	High schools	.48	-.09	.54	-.18	.51
	junior high schools	.45	-.1	.52	-.2	.55
	train stations	.52	-.05	.6	-.14	.34
	hospitals	.45	-.09	.53	-.18	.37
	listed companies	.64	.13	.7	.04	.4
	population	.43	-.13	.51	-.23	.44

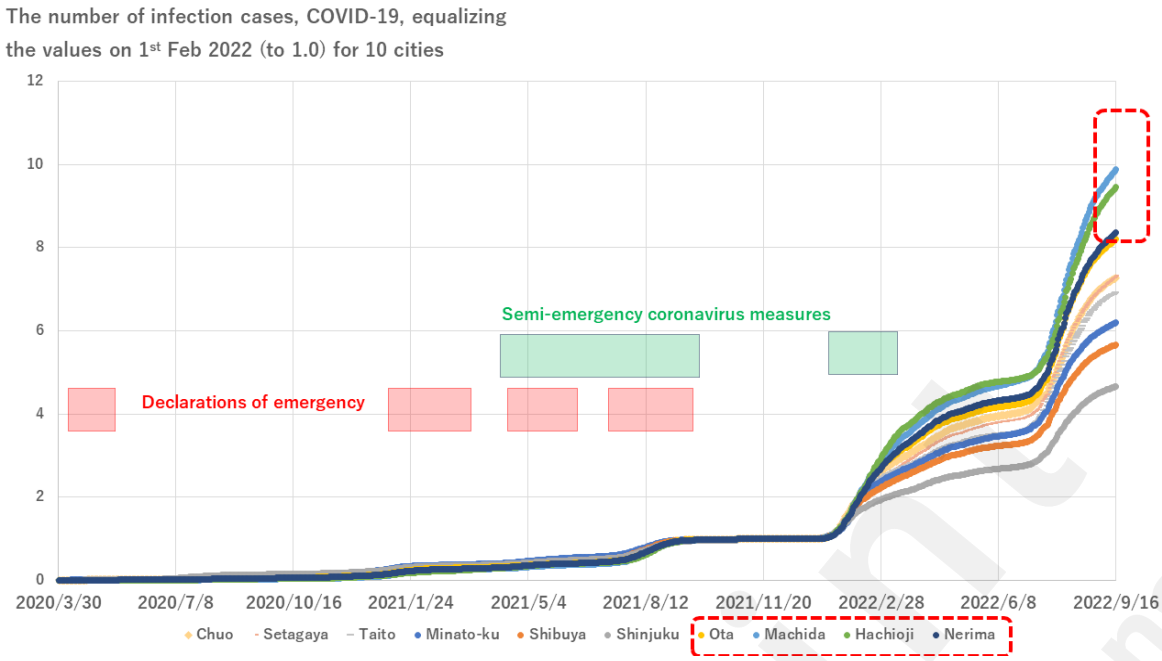

Figure 3. The transition of the number of infection cases for 10 randomly selected municipalities in Tokyo. Because the value is equalized in the period of the most frequent declarations of emergency (by 2021 in Fig.S1), the most radical uptrends in Ota, Machida, Hachioji, and Nerima in this figure (in the dotted frames) show their expansion after the declaration. These regions are of high-rank MDE and low-rank density of restaurants (column BU in the worksheet “Table 1 Indices and cases” in the Generated Dataset 1 (in the Multimedia Appendix 1). Here, we do not show the error bars because the curves only show the raw data.

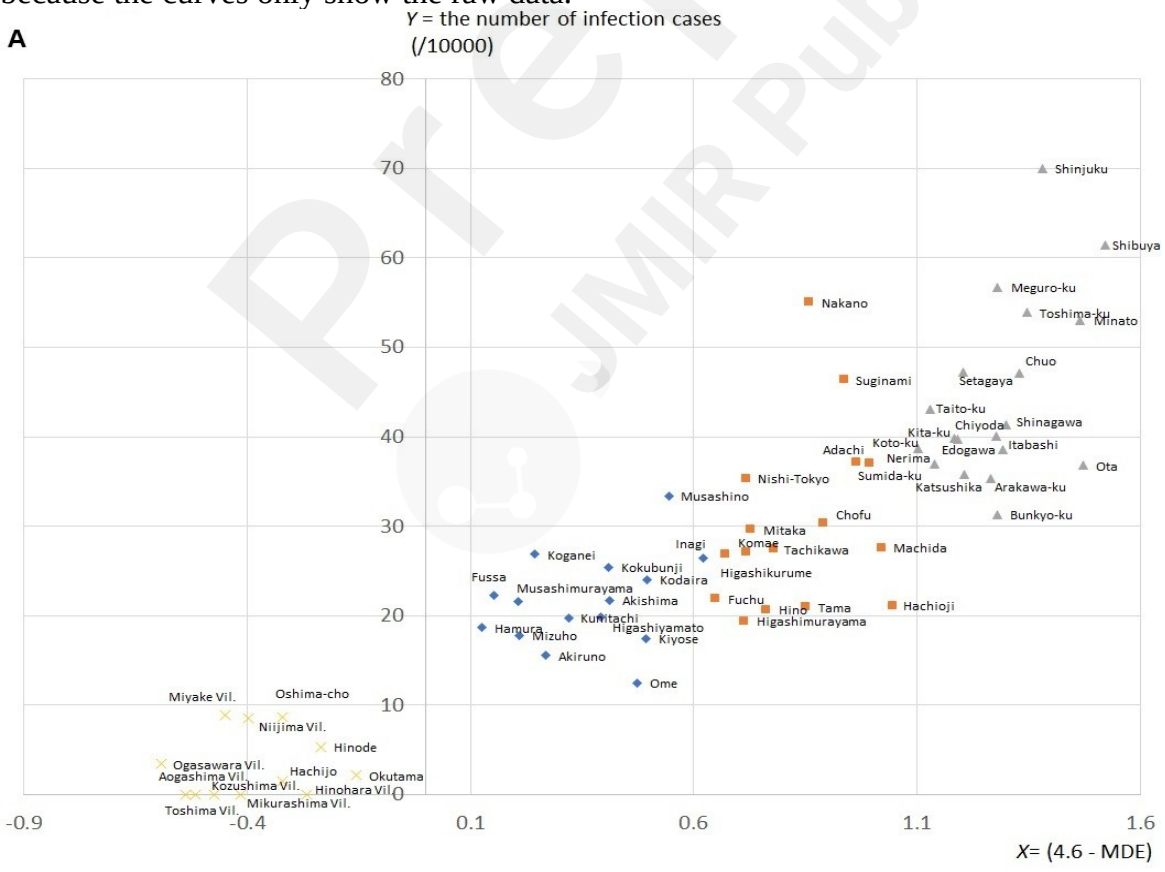

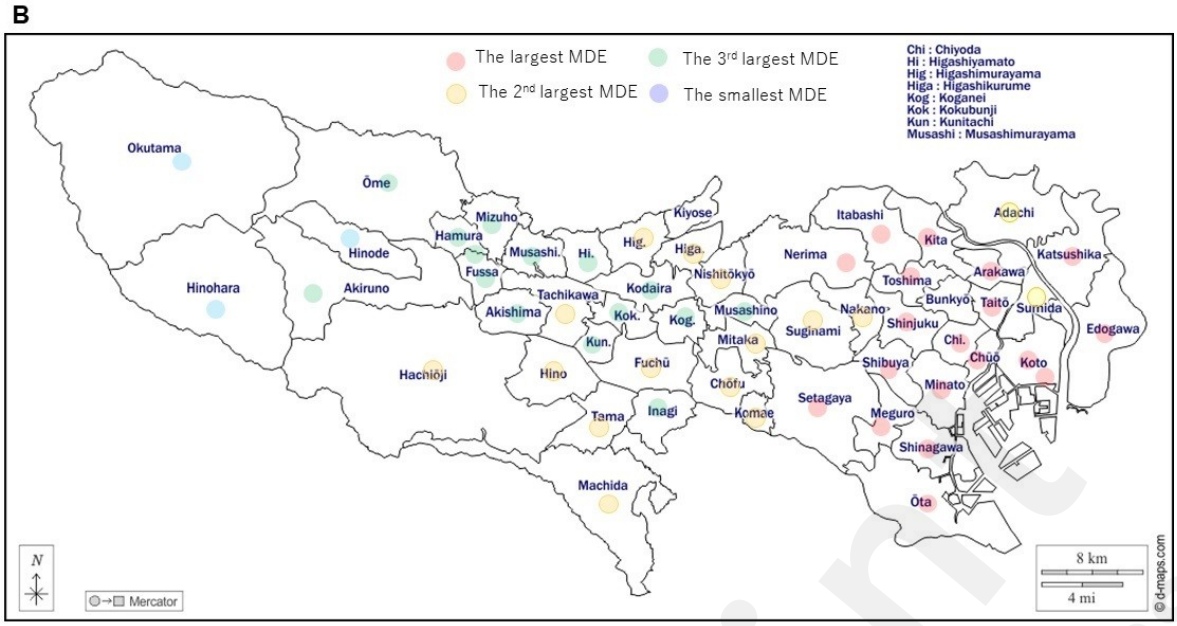

Figure 4. **A**. Distribution of (*X*, *Y*) in Fig. 2**A** in local regions, **B**. their locations in the map: The plots in **A** are clustered corresponding to the colored regions in **B**, that is, the most active part in the east, the next most active part, and the least. Here, **A** includes islands in the lowest cluster to show comparability with Okutama, Hinohara, and Hinode, which are furthest from the central part. Using a free-license map Tokyo free map in [46].

Discussion

Principal Results

The correlation of the MDE with the rate of COVID-19 cases was larger than that of the other factors in Table 2, although it was not significantly larger than that of restaurant density. This strong correlation provides useful information for creating government measures. That is, mobility in and to restaurants has already been restrained by governmental measures such as the declaration of emergency, but MDE has been left without attention. As a result, a significantly rapid expansion in cities with high-rank MDE and low-rank restaurant densities was found, as shown in Fig.3. This shows the necessity of adding the MDE as an index to evaluate the regional latent risk of infection spread.

Because MDE is regarded as an index representing the extent to which individuals from different communities contact each other, the relative weakness of the correlation of MDE with cases of influenza and STDs compared with COVID-19 coincides with Hypothesis A, considering their infectivity with respect to Fig.1**A/C** and **B/D**. That is, Fig. 1**A** and **C** imply that a stronger trend of inter-community infectious contacts accelerates the spread of the virus if it is highly infective, whereas such an acceleration is not observed in Fig.1**B** or **D** for less infective viruses. This also coincides with Fig.4**A**, where the upper-right cluster corresponds to the busiest regions, including the wards in central Tokyo, as shown in Fig.4**B**. In contrast, the lower-left cluster in Fig. 4**A** has the lowest MDE and the lowest number of infected cases and includes the western (low-population) part of Tokyo and the islands.

The transition of MDE implies an improvement or worsening of the behavior of individuals in local regions concerning the spread of infection. The local regions in Classes 1 and 2 in **A**, **B**, and **C** in Fig.5 have large MDEs, corresponding to the upper cluster in Fig.4**A**, while those in Class 3 of the lower MDEs correspond to the lower cluster in Fig.4**A** including the western part of Tokyo, as shown in Fig.4**B** and the islands belonging to Tokyo. However, the regions with the largest

densities of daytime population and influx (moving from other regions) population experienced an upward trend in MDE, as in Class 1 of Fig.5**B** and **C** (especially **B**), during the COVID-19 expansion period that started in the spring of 2020 and remained stable from the summer of 2020 (see also Fig.S1) until July 2021. Such a coincidence between the expansion period and the upward trend of the MDE is not obvious in Fig.5**A** where Class 1 does not show an upward trend, and Class 2 does not show a more obvious downward trend than Class 1. Thus, the accelerated dynamic movements of individuals fostered the interaction of communities, corresponding to an increase in MDE. In addition, individuals in the active regions were found to take fewer safe actions during risky periods, as shown by the upward trends of the MDE in Class 1 of Fig.5**B** and **C**.

Figure 5. Transition of MDE in local regions classified according to population density (**A**: permanent, **B**: daytime, **C**: influx flow). In **B** and **C**, MDE in Class 1 increased during the period of COVID-19 infection expansion. Individuals in cities with high interregional activities are believed to stay careful in these periods, avoiding densely populated areas, but their movements were against their careful attitudes, according to the results here. Note: We do not show error bars as

of MDE (*X-axis*) for the reason discussed in “MDE” of Methods.

Note that we evaluated the correlation between MDE and the spread of infection, but we do not claim to have verified a causal relationship. We proposed MDE as an index for assessing the risk of infection ex post facto from the data by showing only the correlation. However, causal relationships have been published so far, including the above-mentioned [33], which showed that an increase in COVID-19 infection reduces the range of movements and their diversity, which is the opposite in the dedication of causality and in its content (i.e., they analyzed the causality from the spread of infection to human movements, whereas here we evaluate the risk of infection spread relevant to human movements, and they show negative causality, whereas we show positive correlation). Thus, the causality to diversity of the movements due to the spread of COVID-19 is unlikely, and the fact that a correlation was found may be regarded as the likelihood that the causality of COVID-19 infection spread due to the diversification of movements is present. However, it should be understood that there is a limitation in being able to determining whether this is indeed a causal relationship, as it would require an interventional method to actually cause the spread of infection that would be ethically unsuitable.

Limitations

The above results should be interpreted with consideration of these limitations. It is debatable whether mobility patterns obtained from a dataset on mobility collected by smartphones may be generalized to the public [47] because smartphone users may not be representative of the changes in mobility of the population as a whole, and their representativeness may vary by location and season, as pointed out by Wellenius et al. [3]. In addition, because of the privacy policy of the provided dataset, we were unable to assess the characteristics of individuals using smartphones, such as age, gender, race, or income of users.

However, currently, data available from smartphones on the approval of owners is one of the most comprehensive and prevalent data. Studies using data such as GPS sensors are a standard approach in the face of these limitations, including the references above and [33, 41] and [18], which restrict the data subjects further to Facebook users. Compared with studies using other digital methods, such as extracting geolocation data from wearable trackers [48, 49] or geotagged social media posts [50], we used data from a wider range of samples. Furthermore, restricting smartphone data is beneficial for users because it enables a simple, automated, widespread, and easy-to-use method for risk assessment in the future. Thus, the fact that the results of this study were obtained from smartphone data implies their usefulness for infection risk assessments as people are expected to continue to possess smartphones in the future.

In addition, we introduced a statistical entropic feature by aggregating movements to generate inferences about dynamics at a regional scale and discarding unknown heterogeneities. This approach may not cope with the limitations pointed out in [30] that the spatial location of the infection may differ from the location of the surveillance system. In Japan, the locations of infection and residence may differ, and the number of infected persons in

the area of residence was surveyed. However, we explain why we obtained high accuracies for MDE in sensing latent risk in this study, even with this limitation, as follows. First, during the COVID-19 expansion period, people changed to living in the local regions of their own residences due to the Stay Home policy and their own cautiousness. Second, regarding the interregional movement that was still taking place, the following discussion implies that it makes sense to observe the correlation between MDE and the number of infected people counted in their residential regions.

Among the mobilities within region *r* that affect the MDE of *r*, the mobility of residents inside *r* is directly related to their own spread of infection. Let us consider an example scenario for comprehension.

(a) As an essential worker, a nurse or a carer living close to (within the same region *r* as) the hospital or house of the patient they support is from a community that is the nurse station or a care support office or his/her own family, which is different from the patient's family. Similarly, a visitor to a family living close to it is from a different family.

On the other hand, the mobility within *r* of those from residents outside *r* also affects a part of the MDE of region *r* because this mobility reflects the diversity of the communities they come into contact with inside and outside *r*.

(b) A nurse or care manager, who lives in *r*‘ and visits a family in *r* ($r \cap r' = \phi$), generates an inter-community interaction because his/her community differs from the family to visit.

Thus, the mobility within *r* of individuals from both inside and outside *r* is related to the spread of infection among the residents of *r*.

We additionally evaluated the influence of the mobility of those living and acting only outside *r* on the spread of infection in region *r* as follows:

(c) A nurse or care manager who lives in one's own region *r'* ($r \cap r' = \phi$) and interact only within *r'* ‘ causes inter-community interactions in *r'* similar to the case of (a). Such individuals are indirectly related to the infection expansion in *r* because they contact other essential workers who visit region *r* as in (b).

Comparison with Prior Work

The point of this paper is *not* to present a "best" index for risk assessment although comparisons with other indices, such as population density, have been made as in Table 1. In fact, the superiority of MDE over population density was not significant (p=.11). Because MDE is an independent measure that is not affected by population density (because MDE is probability-based), we propose combining MDE with other indices, including population density, rather than choosing a better index. Such a combinatorial use of indices is essential for risk assessment and protective policies in the future, in such a way as "this city has low population density, small number of supermarket, etc., but MDE is high. So, citizens should be careful!" or "most people wear masks in this city, but MDE is high. We should consider measures other than masks and urge citizens to take vaccines." Because MDE is only a statistical indicator about the likeliness of infection spread, based on the probability of moving direction, combining it with other indices is an essential approach toward finer risk assessment. In this sense, MDE is also expected to be used as a variable to reinforce the approach of using similar mobility data [51] or multivariate machine learning [52] and further improve the accuracy of the prediction of infection cases.

From a technical perspective, mobility-based studies on the spread of infection using sensors such as GPS in smartphones are geographically restricted. For example, [33] was limited to smartphone owners in four cities in northern Thailand, [50] to geolocated SNS users in New York City, [53] to

the city of El Pasto in Texas, and [54] to parks in the US. Compared with these studies, Tokyo is a large city with 14 million inhabitants, and the 53 municipalities range from urban to mountainous areas with very small populations, including regions of various pre-pandemic periods (2019 in all regions in Tokyo, and even until the end of 2020 in suburbs such as Kokubunji, Kunitachi, Inagi, and Hamur, and all regions found severe outbreaks in 2022), thus including regions of diverse situations. Thus, the data used in this study are suitable for our attempts to derive laws not limited to activities in particular industries or regions.

Compared with the approach of the Three Cs applied in Japan during the pandemic period [55, 56], where individuals were forbidden to meet in a closed space, crowded place, or close-contact settings, the measure to reduce MDE can be applied to realize secure movements rather than a way of staying in a meeting place.

However, controlling human mobility in urban transit [57, 58] could not necessarily be regarded as an effective method for suppressing the spread of COVID-19 pandemic because urban transit may not have a stronger influence on the spread than mobility in groceries and pharmacies [59]. These results coincide with those in Table 2, where the number of train stations had a weaker correlation with the number of infections than did supermarkets.

Note again that the regions are colored independently of the population or its density because they depend only on the values of the MDE obtained from the sheer probabilistic distribution of the movement directions of individuals. We should recollect the better fitness of the MDE than the population density of these locations, as shown in Table 2, which sheds light on the controversy regarding the impact of the population density [11].

Conclusions

In this paper, we showed four essential findings. First, the MDEs for local regions showed significant invariance between different periods from before to within the COVID-19 pandemic period. Second, MDE was found to be significantly correlated with the rate of infection cases of COVID-19 over local populations in the 53 inland regions of Tokyo. The correlation with MDE was higher for COVID-19 than for influenza, which was higher than that of STD, that is, in the order of infectivity of the virus. This supports the hypothesis that the impact of inter-community contact on infection expansion increases for a virus with higher infectivity. Third, the spread of COVID-19 was accelerated in regions with high-rank MDEs compared to those with high-rank restaurant densities during and after the period of governmental declarations of emergency. Fourth, the MDEs tended to be high and increased during the COVID-19 period in regions where influx or daytime movement was active.

A possible explanation of the third and fourth findings above is that policymakers and living people have been overlooking risk factors corresponding to MDE, even during governmental declarations of emergency. Furthermore, the infection-suppression effort and its effect on sheer reduction of movements tend to weaken significantly after the relaxation of strict control measures [60]. Thus, we propose to keep monitoring MDE values and, if MDE increases, send out messages to satisfy the constraint on intercommunity contacts, such as the SWYC guidelines, or to keep cautious in visiting a place where people move in diverse directions. However, we did not consider controlling individual movements as the main measure because it would be difficult for a single person to lead the movements of others. Thus, we regard it as a practical use of MDE to improve the social environment, such as the development of pathways and other infrastructure to unify the direction of pedestrian movement in urban areas, where possible. If individual behaviors are to be controlled, it should only be added as a supplementary message to environmental improvements, such as encouraging people to wear masks in areas where there is inevitably a diversity of directions of movement or to avoid visiting places where people move in various directions. In addition, it is difficult from a research ethics perspective to analyze data on individual movements.

However, we propose an application of MDE to visualize the locations of high-risk regions to accelerate the awareness of both individuals and society as a whole regarding the risks in local regions. Individuals living or working in regions highlighted in the heatmap of the MDE, as shown in Fig.6, will enhance their risk awareness, and their communication will enhance the awareness of regional society. In Fig. 6**A** and **B**, 100m square meshes with the highest MDE in Tokyo are shown in dense red (1000 meshes in Tokyo with the highest MDE values), and weaker colors represent the ranks of meshes on their MDE values. Despite cancelling the effects of city size and human crowd as discussed above, the dense red areas in Fig.6**A** and squares in Fig.6**B** clustered close to the busiest stations (**A**: in the central wards Shibuya, Shinjuku, et al, **B**: in a selected ward Bunkyo). The mesh regions of the highest MDE do not necessarily coincide with train stations, but some coincide with supermarkets and restaurants, which corresponds to the literature [59].

A

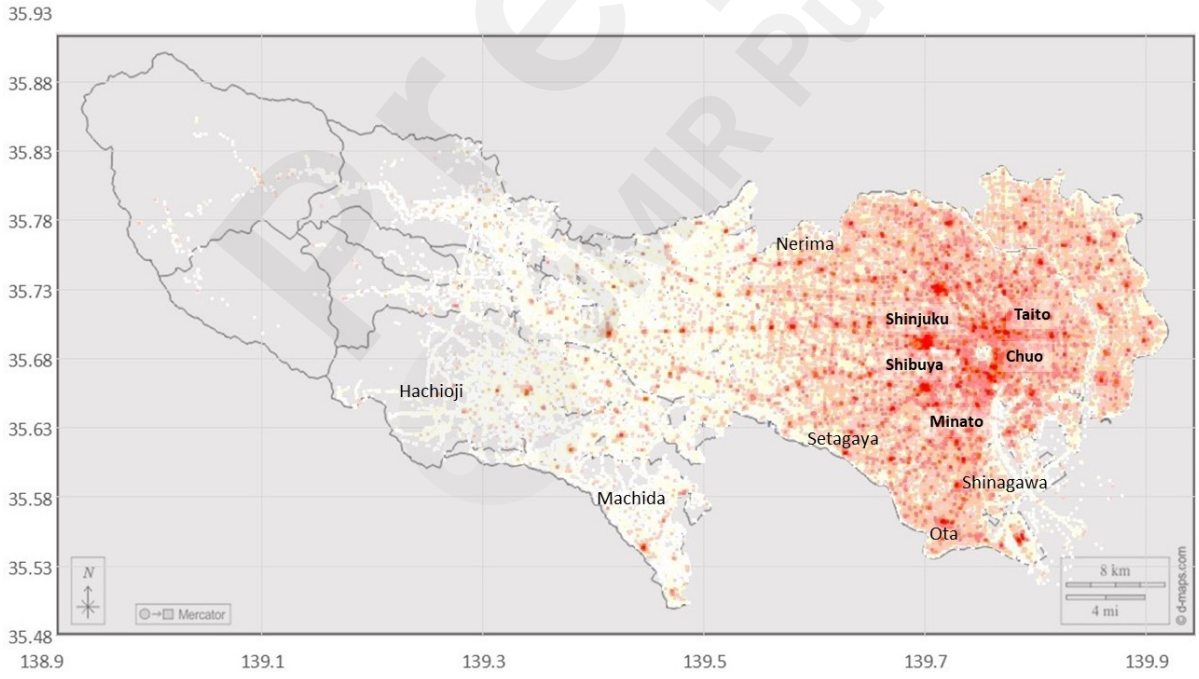

B

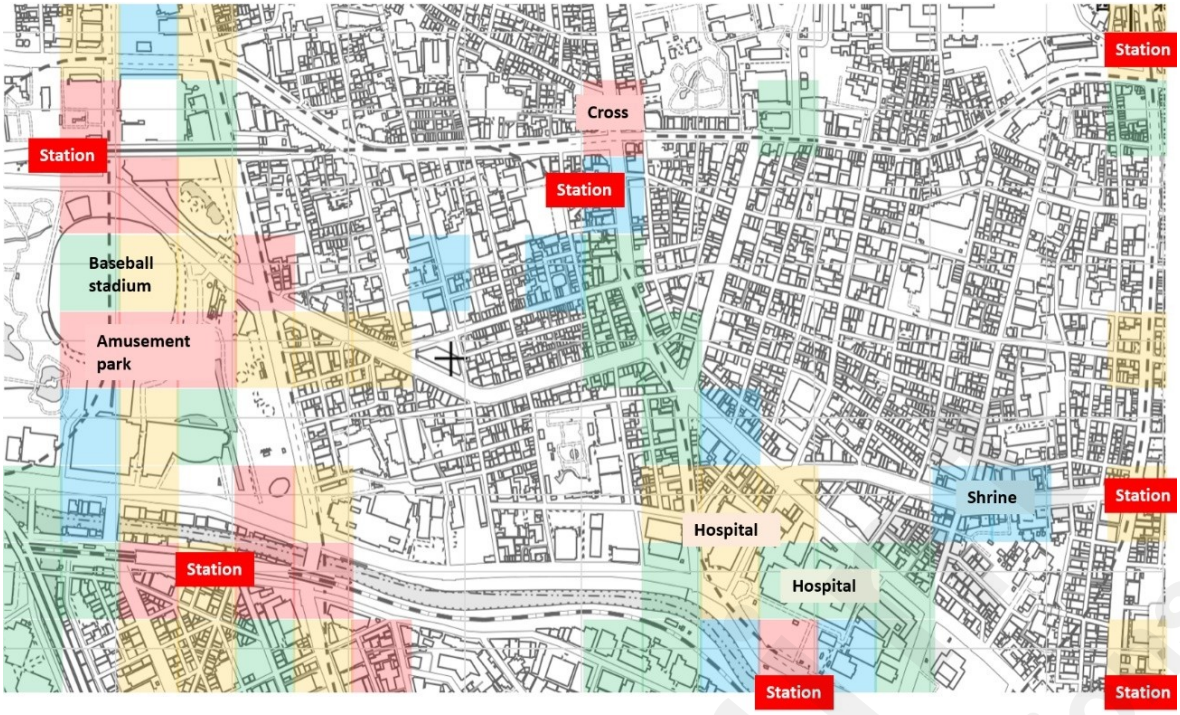

Figure 6. The heatmaps of MDE for 100m meshes in **A**: all Tokyo except islands and **B**: a part of Bunkyo-ward near the University of Tokyo. Meshes are classified on the MDE values (red: top 1000 meshes in Tokyo, yellow: the second top 1000 meshes, green: the third, blue: the fourth). All use free-license maps: **A:** Tokyo free map [46], **B:** Blank maps from the Geospatial Information Authority of Japan [61]

Acknowledgements

This study was supported by the JST Grant JPMJPF2013, Q-Leap JPMXS0118067246, JSPS Kakenhi 20K20482, 23H00503, MEXT Initiative for Life Design Innovation, and the Cabinet Secretariat of Japan. The funders played no role in the study design, data collection and analysis, decision to publish, or manuscript preparation. We used Paperpal.com only for checking and correcting English expressions.

Data Availability Statement

Research data supporting this publication and its links are available in the manuscript (datasets in the Methods section and Multimedia Appendix 1).

However, the device location data given as the Used Dataset 1 are *not publicly available* because of the contract between Agoop Corp. and the authors who analyzed the data, but may be made available upon reasonable request if both the authors and Agoop Corp. agree to data sharing. The data on infection cases (Used Dataset 2), regional population (Used Dataset 3), and institutions (Used Dataset 4) are publicly available and are provided in the Supporting Information. The processed data on the MDE using the Used Dataset 1 are available in Multimedia Appendix 1.

Ethical considerations

The data on human movements in Tokyo, referred to the Used Dataset 1, were smartphone-derived mobility data collected preventing identification of individual users by Agoop Corporation. The subjects provided their consent before data collection. The procedures for data collection and avoidance of the risk of personal identification were performed in accordance with the Japanese Act on the Protection of Personal Information [62] and the guidelines of the Location Business and Marketing Association of Japan [63]. This dataset does not constitute a clinical trial or involve

human subjects research, and is widely available for both commercial and academic research use upon purchase [51, 64, 65], which verifies that the use in this study is supported ethically by established use cases. The authors purchased the data for academic research use and obtained permission to use.

The collection of this dataset was approved in the review of the internal committee of Agoop Corp. for privacy protection and compliance management. Then, the exemption of the ethical review on this data collection and the present secondary analysis were both approved by the Institutional Review Board (IRB) of Medical Governance Research Institute (Tokyo, Japan) (no. 22000031)

Furthermore, the present secondary analysis is exempt from an IRB review in accordance with the Ethical Guidelines for Medical and Health Research Involving Human Subjects of the Ministry of Health, Labour and Welfare, Japan [66] . The analyses on the Used Dataset 1 were also approved as an exemption by the Research Ethics Committee of School of Engineering,, The University of Tokyo (ref no.24-23).

Conflicts of Interest

The authors have declared that no competing interests exist.

Abbreviations

SWYC: Staying with One's Community
MDE: Movement Direction Entropy

Reference

1 Patterson S. The Politics of Pandemics: The Effect of Stay-At-Home Orders on COVID-19 Mitigation. *State Politics & Policy Quarterly* 2021; **22**(1): 1-23. doi:10.1017/spq.2021.14

2 Lurie MN, Silva J, Yorlets RR, et al. Coronavirus Disease 2019 Epidemic Doubling Time in the United States Before and During Stay-at-Home Restrictions, *J. Infect. Dis.* 2020; **222** (10): 1601–1606, doi: 10.1093/infdis/jiaa491

3 Wellenius G.A., Vispute S., Espinosa V. et al. Impacts of social distancing policies on mobility and COVID-19 case growth in the US. *Nat. Commun.* 2021; **12**: 3118. https://doi.org/10.1038/s41467-021-23404-5

4 Park S, Michelow IC, Choe YJ, Shifting Patterns of Respiratory Virus Activity Following Social Distancing Measures for Coronavirus Disease 2019 in South Korea. *J. Infect. Dis.* 2021; **224** (11):1900–1906, doi: 10.1093/infdis/jiab231

5 Lim JT, Chew LZX, Choo ELW, et al. Increased Dengue Transmissions in Singapore Attributable to SARS-CoV-2 Social Distancing Measures, *J. Infect. Dis.* 2021; **223** (3): 399–402, doi: 10.1093/infdis/jiaa619

6 Deng W, Xie H, Creighton M. Li BY. Patterns of violence and mental health outcomes characterizing vulnerability in SGM college students before and during the COVID-19 pandemic *Nat. Mental Health.* 2023; **1**: 564–572. doi: 10.1038/s44220-023-00097-x

7 Aknin LB, Andretti B, Goldszmidt R et al. Policy stringency and mental health during the COVID-19 pandemic: A longitudinal analysis of data from 15 countries. *Lancet.* 2022; 7(5): 417–426. doi: 10.1016/S2468-2667(22)00060-3

8 Plett D., Pechlivanoglou, P. & Coyte, P. C. The impact of provincial lockdown policies and COVID-19 case and mortality rates on anxiety in Canada. *Psychiatry Clin. Neurosci.* 2022 doi: 10.1111/pcn.13437

9 Nivette A.E., Zahnow R., Aguilar R. et al. A global analysis of the impact of COVID-19 stay-at-home restrictions on crime. *Nat Hum Behav* 2021; 5: 868–877. doi: 10.1038/s41562-021-01139-z

10 Béland, L.P., Brodeur, A., Wright, T., The Short-Term Economic Consequences of COVID-19: Exposure to Disease, Remote Work and Government Response, *Plos ONE* 2023; **18** (3): e0270341 doi:10.1371/journal.pone.0270341

11 Khavarian-Garmsir AR, Sharifi A, Moradpour N. Are high-density districts more vulnerable to the COVID-19 pandemic? *Sustain. Cities Soc.* 2021; **70**: 102911 doi:10.1016/j.scs.2021.102911

12 Ohsawa Y, Tsubokura M. Stay with your community: Bridges between clusters trigger expansion of COVID-19. *PLoS ONE* 2020; **15** (12): Article e0242766, 10.1371/journal.pone.0242766

13 Cabinet Secretariat Big Data drives Japan's Pandemic Response Strategies. Big data drives Japan's pandemic response strategies, Lessons taken from data and scientific models could improve future policy. *Nature.* 2023. https://www.nature.com/articles/d42473-023-00185-7

14 Ohsawa Y, Kondo S. Regional Workshop for Policy Implementation Based on the Stay with Your Community Principles, *Proc. Comp. Sci*. 2022; **207**: 3057-3064 doi: 10.1016/j.procs.2022.09.363.

15 Leng T, White C, Hilton J et al. The effectiveness of social bubbles as part of a Covid-19 lockdown exit strategy, a modelling study, *Welcome Open Res*. 2021; **5**:213. doi:10.12688/wellcomeopenres.16164.2.

16 Sigler T, Mahmuda S, Kimpton A et al. The socio-spatial determinants of COVID-19 diffusion: the impact of globalisation, settlement characteristics and population. *Glob. Health.* 2021; **17**: 56, doi: 10.1186/s12992-021-00707-2. PMID: 34016145.

17 Neiderud CJ. How urbanization affects the epidemiology of emerging infectious diseases. *Infection Ecology & Epidemiology* 2015; **5**(1): doi: 10.3402/iee.v5.27060

18 Kishore, N. et al. Lockdowns result in changes in human mobility which may impact the epidemiologic dynamics of SARS-CoV-2. *Sci. Rep.* 2021; **11**: 6995. doi: 10.1038/s41598-021-86297-w

19 Eubank S, Guclu H, Kumar AVS et al. Modelling disease outbreaks in realistic urban social networks. *Nature* 2004; 429:180–184. pmid:15141212, https://doi.org/10.1038/nature02541

20 Liu M, Li D, Qin P, Liu C, Wang H, Wang F. Epidemics in interconnected small-world networks. *PLoS ONE.* 2015;**10**(3): e0120701. Available from: https://journals.plos.org/plosone/article?id=10.1371/journal.pone.0120701 pmid:25799143View ArticlePubMed/NCBIGoogle Scholar

21 Thurner, S., Klimek, P. & Hanel, R. A network-based explanation of why most COVID-19 infection curves are linear. *Proc. Natl. Acad. Sci.* 2020; **117**(37): 22684–22689. doi: 10.1073/pnas.2010398117

22 Della Rossa, F., Salzano, D., Di Meglio, A. et al. A network model of Italy shows that intermittent regional strategies can alleviate the COVID-19 epidemic. *Nat. Commun.* 2020; **11**: 5106. . doi: /10.1038/s41467-020-18827-5

23 Xue D, Hirche S. Distributed topology manipulation to control epidemic spreading over networks. *IEEE Trans. Signal Proc.* 2019; **67**: 1163–1174.

24 Wylie, JL, Cabral T, Jolly AM, Identification of Networks of Sexually Transmitted Infection: A Molecular, Geographic, and Social Network Analysis, *J. Infect. Dis.* 2005, **191** (6); 899–906, . doi: 10.1086/427661

25 Schneeberger A, Mercer C, Gregson SA et al. Scale-free networks and sexually transmitted diseases: a description of observed patterns of sexual contacts in Britain and Zimbabwe. *Sex Transm Dis.* 2004; **31**(6):380–387. pmid:15167650

26 Shannon CL, Klausner JD. The growing epidemic of sexually transmitted infections in adolescents: a neglected population. *Current Opinion in Pediatrics* 2018; **30**(1): 137-143, doi:10.1097/MOP.0000000000000578

27 Bai Y, Tao X. Comparison of COVID-19 and influenza characteristics. *Zhejiang Univ Sci B* 2021; **22**(2): 87–98. doi: 10.1631/jzus.B2000479

28 Xue L, Jing S, Zhang K et al. Infectivity versus fatality of SARS-CoV-2 mutations and influenza. *Int'l J. Infect. Dis.* 2022. **121**: 195-202. doi: 10.1016/j.ijid.2022.05.031

29 Daemi HB, Kulyar MF, He X et al. Progression and Trends in Virus from Influenza A to COVID-

19: An Overview of Recent Studies. *Viruses* 2021; 13(6):1145. doi: 10.3390/v13061145
30 Wesolowski A, Buckee CO, Engø-Monsen K et al. Connecting Mobility to Infectious Diseases: The Promise and Limits of Mobile Phone Data, *J. Infect. Dis.* 2016; **214** (4): S414–S420. doi: 10.1093/infdis/jiw273
31 Santana C., Botta F., Barbosa H. et al. COVID-19 is linked to changes in the time–space dimension of human mobility. *Nat. Hum. Behav.* 2023. doi: 10.1038/s41562-023-01660-3
32 Abdul-Ghani R, Fouque F, Mahdy MAK et al. Multisectoral Approach to Address Chikungunya Outbreaks Driven by Human Mobility: A Systematic Review and Meta-Analysis, *J. Infect. Dis 2020:* **222** (S8):S 709–S716. doi:10.1093/infdis/jiaa500
33 Haddawy, P. et al. Effects of COVID-19 government travel restrictions on mobility in a rural border area of Northern Thailand: a mobile phone tracking study. *PLoS ONE* 2021; **16**: e0245842
34 Fan, C., Lee, R., Yang, Y. & Mostafavi, A. Fine-grained data reveal segregated mobility networks and opportunities for local containment of COVID-19. *Sci. Rep.* 2021; **11**: 16895
35 Ahern, J. From fail-safe to safe-to-fail: Sustainability and resilience in the new urban world. *Landsc. Urban Plann.* 2011; **100**: 341–343. doi: j.landurbplan.2011.02.021
36 Cumming, G. S., Olsson, P., Chapin, F. & Holling, C. Resilience, experimentation, and scale mismatches in social-ecological landscapes. *Landsc. Ecol.* 2013; **28**: 1139–1150. doi: 10.1007/s10980-012-9725-4
37 Marcus, L. & Colding, J. Toward an integrated theory of spatial morphology and resilient urban systems. *Ecol. Soc*. 2014; **19**(4), 55
38 Wang, H., Ghosh, A., Ding, J. et al. Heterogeneous interventions reduce the spread of COVID-19 in simulations on real mobility data. *Sci Rep* 2021; **11**: 7809. doi: 10.1038/s41598-021-87034-z
39 Wang HY, Yamamoto N. Using a partial differential equation with Google Mobility data to predict COVID-19 in Arizona. *Math. Biosci. Eng.* 2020; **17**: 4891–4904 doi: 10.3934/mbe.2020266
40 Wang S, Tong Y, Fan Y, Liu H, Wu J, Wang Z., Fang C. Observing the silent world under COVID-19 with a comprehensive impact analysis based on human mobility. *Sci. Rep.* 2021; **11**: 14691. doi: 10.1038/s41598-021-94060-4
41 Cot, C., Cacciapaglia, G. & Sannino, F. Mining Google and Apple mobility data: temporal anatomy for COVID-19 social distancing. *Sci. Rep.* 2021; **11**: 4150. doi: 10.1038/s41598-021-83441-4
42 Oh, J. et al. Mobility restrictions were associated with reductions in COVID-19 incidence early in the pandemic: evidence from a real-time evaluation in 34 countries. *Sci. Rep.* 2021; **11**: 13717. doi: 10.1038/s41598-021-92766-z
43 Lenormand, M. et al. Entropy as a measure of attractiveness and socioeconomic complexity in Rio de Janeiro metropolitan area. *Entropy* 2020; **22**; 368. doi: 10.3390/e22030368
44 Pappalardo, L. et al. An analytical framework to nowcast well-being using mobile phone data. Int. J. Data Sci. Anal. 2016; **2**: 75–92. doi: 10.1007/s41060-016-0013-2
45 Gallotti, R., Bazzani, A., Degli Esposti, M. & Rambaldi, S. Entropic measures of individual mobility patterns. *J. Stat. Mech. Theory Exp.* 2013, P10022. doi: 0.1088/1742-5468/2013/10/p10022 (2013).
46 Tokyo free map https://d-maps.com/carte.php?num_car=132337&lang=en,
47 Huang, X. et al. The characteristics of multi-source mobility datasets and how they reveal the luxury nature of social distancing in the U.S. during the COVID-19 pandemic. Int. J. Digital Earth 14, 424–442 (2021), doi: 10.1080/17538947.2021.1886358.
48 Patnode, C.D., Lytle, L.A., Erickson, D.J., Sirard, J.R., Barr-Anderson, D., Story, M., The relative influence of demographic, individual, social, and environmental factors on physical activity among boys and girls, Int'l J. of Behavioral Nutrition and Physical Activity 7 (2010), 1-10, 10.1186/1479-5868-7-79
49 Tappe, K.A.., Glanz, K., Sallis, J.F., Zhou, C., Saelens, B.E., Children's physical activity and parents' perception of the neighborhood environment: Neighborhood impact on kids study, Int'l J.

of Behavioral Nutrition and Physical Activity 10 (2013), 1-10, 10.1186/1479-5868-10-39
50 Hamstead, Z.A., Fisher, D., Ilieva, R.T., Wood, S.A., McPhearson, T., Kremer, P., Geolocated social media as a rapid indicator of park visitation and equitable park access, Computers, Environment and Urban Systems 72 (2018), pp. 38-50, 10.1016/j.compenvurbsys.2018.01.007.
51 Kato H, Takizawa A., Time series cross-correlation between home range and number of infected people during the COVID-19 pandemic in a suburban city. PLoS ONE 17(9) (2022), e0267335. https://doi.org/10.1371/journal.pone.0267335
52 Garcia-Cremades S. et al. Improving prediction of COVID-19 evolution by fusing epidemiological and mobility data. *Sci. Rep.* 2021; 11: 15173. doi: 10.1038/s41598-021-94696-2
53 Song, Y., Lee, S., Park, A. H., & Lee, C. (2023). COVID-19 impacts on non-work travel patterns: A place-based investigation using smartphone mobility data. Environment and Planning B: Urban Analytics and City Science, 50(3), 642-659. https://doi.org/10.1177/23998083221124930
54 Jay J, Heykoop F, Hwang L, Courtepatte A, de Jong J, Kondo M. Use of smartphone mobility data to analyze city park visits during the COVID-19 pandemic. Landsc Urban Plan. 2022 Dec;228:104554. doi: 10.1016/j.landurbplan.2022.104554. Epub 2022 Sep 6. PMID: 36091471; PMCID: PMC9444487.
55 Allgayer, S., Kanemoto, E. The <Three Cs> of Japan's Pandemic Response as an Ideograph. Front. Commun. 2021; 6:595429. doi: 10.3389/fcomm.2021.595429
56 The Government of Japan. Avoiding the Three Cs: A Key to Preventing the Spread of COVID-19. KIZUNA: Linking Japan and the World. Dec 24, 2020. https://www.japan.go.jp/kizuna/2020/avoiding_the_three_cs.html
57 Li Y, et al. The Impact of Policy Measures on Human Mobility, COVID-19 Cases, and Mortality in the US: A Spatiotemporal Perspective. *Int. J. Environ. Res. Public Health* 2021; **18**(3): 996 . doi: 10.3390/ijerph18030996
58 Vokó Z, Pitter JG. The effect of social distance measures on COVID-19 epidemics in Europe: an interrupted time series analysis. *GeroScience*. **2020**; 42: 1075–1082. doi: 10.1007/s11357-020-00205-0
59 Kato H, Takizawa A. Human mobility and infection from Covid-19 in the Osaka metropolitan area. npj *Urban Sustain.* 2022; **2**: 20. doi: 10.1038/s42949-022-00066-w
60 Nouvellet P et al. Reduction in mobility and COVID-19 transmission. *Nat. Commun.* 2021; **12**, 1090. doi: 10.1038/s41467-021-21358-2
61. Agoop Corp. Collection and deidentification of the device location data. https://agoop.co.jp/service/data-usage-policy/
62 LABA Japan. The guideline for device location data. https://www.lbmajapan.com/guideline
63 Shida, Y., Ozaki, J., Takayasu, H. et al. Potential fields and fluctuation-dissipation relations derived from human flow in urban areas modeled by a network of electric circuits. Sci Rep 12 (2022), 9918, https://doi.org/10.1038/s41598-022-13789-8
64 Nagata, S., Nakaya, T., Hanibuchi, T. et al. Development of a method for walking step observation based on large-scale GPS data. Int J Health Geogr 21 (2022). 10, https://doi.org/10.1186/s12942-022-00312-5
65 Ministry of Health, Labor, and Welfare of Japan. Ethical Guidelines for Medical and Health Research Involving Human Subjects from the Ministry of Health. https://www.mhlw.go.jp/content/001077424.pdf
66 Geospatial Information Authority of Japan, Geographical Survey Institute Map Vector (in Japenese) https://maps.gsi.go.jp/vector/
67 Tokyo Metropolitan Government. Number of positive cases of novel coronavirus infection by ward, city, town, and village, 2022.

"https://spec.api.metro.tokyo.lg.jp/spec/t000010d0000000085-2215a7dcc2ff9f2a535063a2d4d42ece-0

68 Tokyo Metropolitan Infectious Disease Surveillance Center, Epidemiological Surveillance of Infectious Diseases, Accessed 2023.
"https://survey.tmiph.metro.tokyo.lg.jp/epidinfo/epimenu.do
69 Tokyo Metropolitan Government. Tokyo Metropolitan government, List of fixed-point medical institutions for investigation of infectious diseases, 2021.
https://idsc.tmiph.metro.tokyo.lg.jp/assets/year/2021/2021-3.pdf
70 Tokyo Metropolitan Government. List of medical institutions with outpatient services, Accessed 2023.
https://www.hokeniryo.metro.tokyo.lg.jp/kansen/corona_portal/soudan/hatsunetsugairai.html.
71 Tokyo Metropolitan Government. Information on medical and pharmacy functions in Tokyo. Accessed 2023.
https://www.himawari.metro.tokyo.jp/qq13/qqport/tomintop/
72 Tokyo Metropolitan Government. Population of Tokyo (population by place of work or school) according to the 2020 census (in Japanese) https://www.toukei.metro.tokyo.lg.jp/tyukanj/2020/tj-20index.htm
73 Apamanshop.com, Regional information of Tokyo (in Japanese), accessed 2023. https://www.apamanshop.com/tokyo/townpage/

Supplementary Files

Untitled.
URL: http://asset.jmir.pub/assets/15d11d00607312de4f8845bc24df397f.docx

Untitled.
URL: http://asset.jmir.pub/assets/88ae341f9dbf4ad4f442cdddbace8fe9.docx

Untitled.
URL: http://asset.jmir.pub/assets/70a626e125254849203a0e02c079643f.docx

Figures

Viral infections spread across two types of networks. A and C: Strong inter-community bridges (for example, COVID-19), B and D: weak inter-community bridges (e.g. STDs). Influenza is positioned as of inter-community bridges of intermediate strength. Meeting places are represented by the orange shadows, as in C and D.

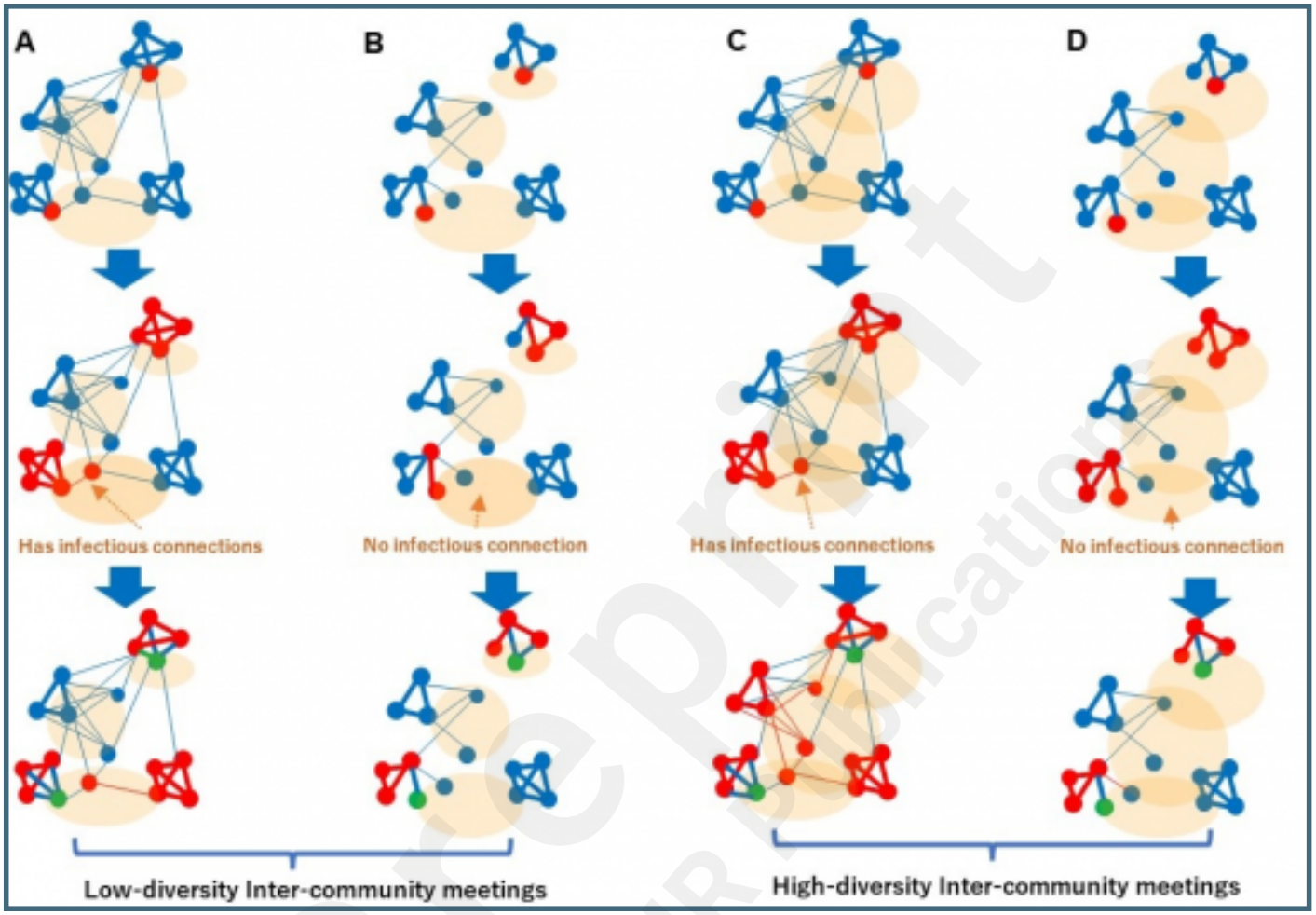

Correlation between X as A: MDE, and the densities (numbers per km2) of B: restaurants, C: supermarkets, and D: hospitals, versus the rates (cases per 104 habitats) of infection cases (Y: COVID-19): The dots represent the values of (X, Y) for the 53 municipalities in Tokyo excluding islands. Note that both values do not reflect the population but are the rates obtained by dividing the number by the width or population of each city. MDE is converted here for visualization to -log?(4.6-H_MDE).

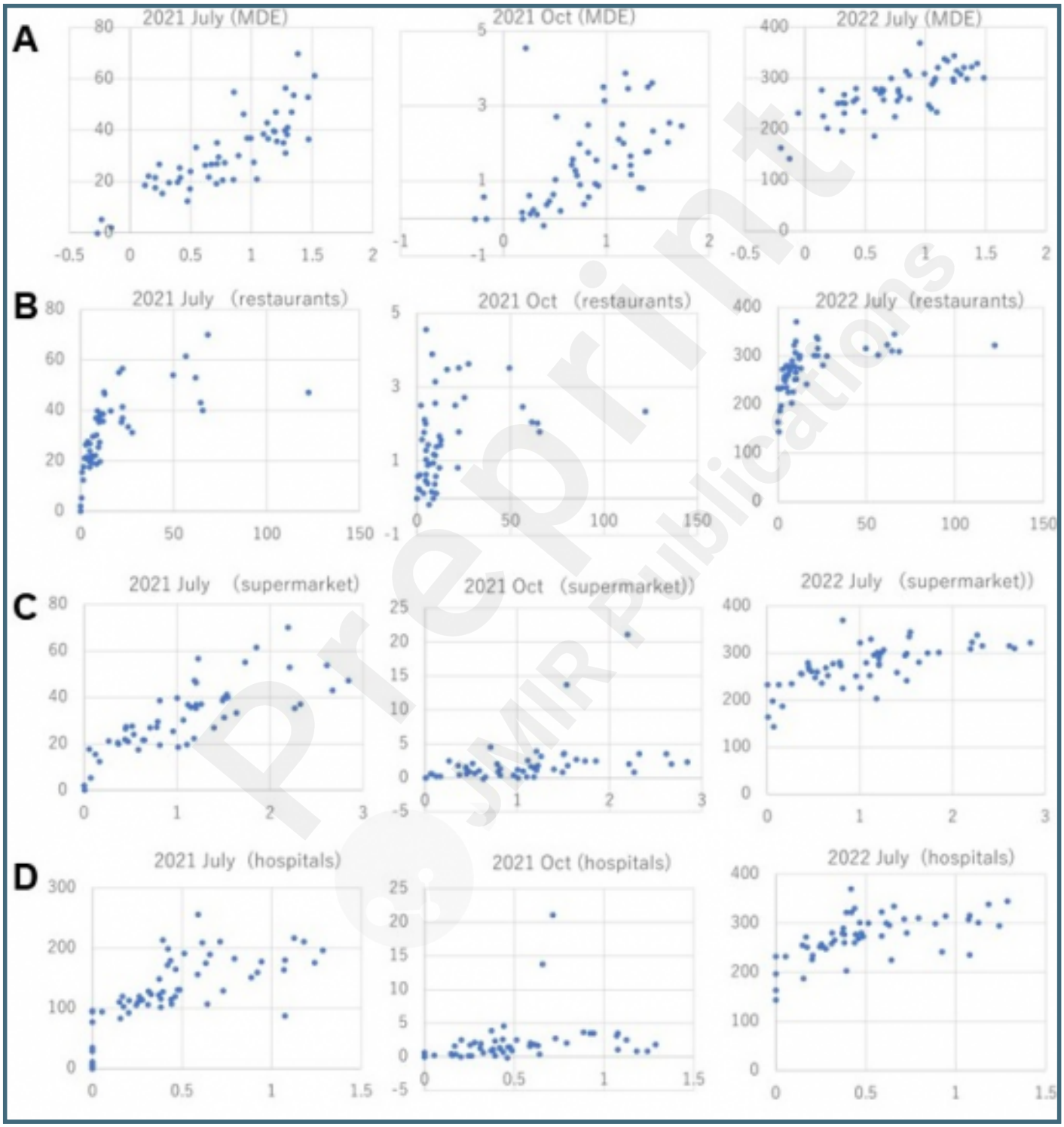

The transition of the number of infection cases for 10 randomly selected municipalities in Tokyo. Because the value is equalized in the period of the most frequent declarations of emergency (by 2021 in Fig.S1), the most radical uptrends in Ota, Machida, Hachioji, and Nerima in this figure (in the dotted frames) show their expansion after the declaration. These regions are of high-rank MDE and low-rank density of restaurants (column BU in the worksheet “Table 1 Indices and cases” in the Generated Dataset 1 (in the Supporting Information). Here, we do not show the error bars because the curves only show the raw data.

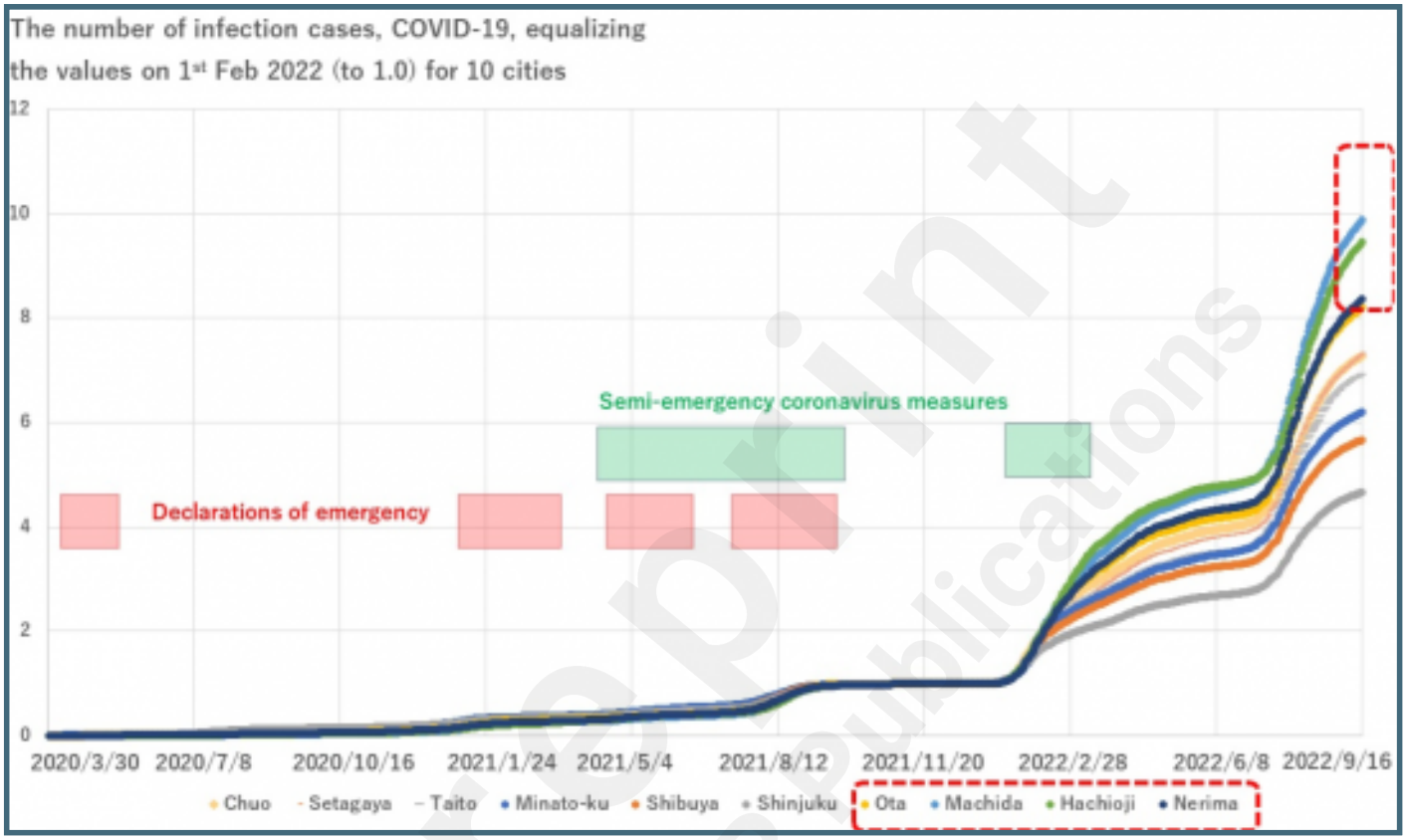

A. Distribution of (X, Y) in Fig. 2A in local regions, B. their locations in the map: The plots in A are clustered corresponding to the colored regions in B, that is, the most active part in the east, the next most active part, and the least. Here, A includes islands in the lowest cluster to show comparability with Okutama, Hinohara, and Hinode, which are furthest from the central part. Using a free-license map Tokyo free map in [46].

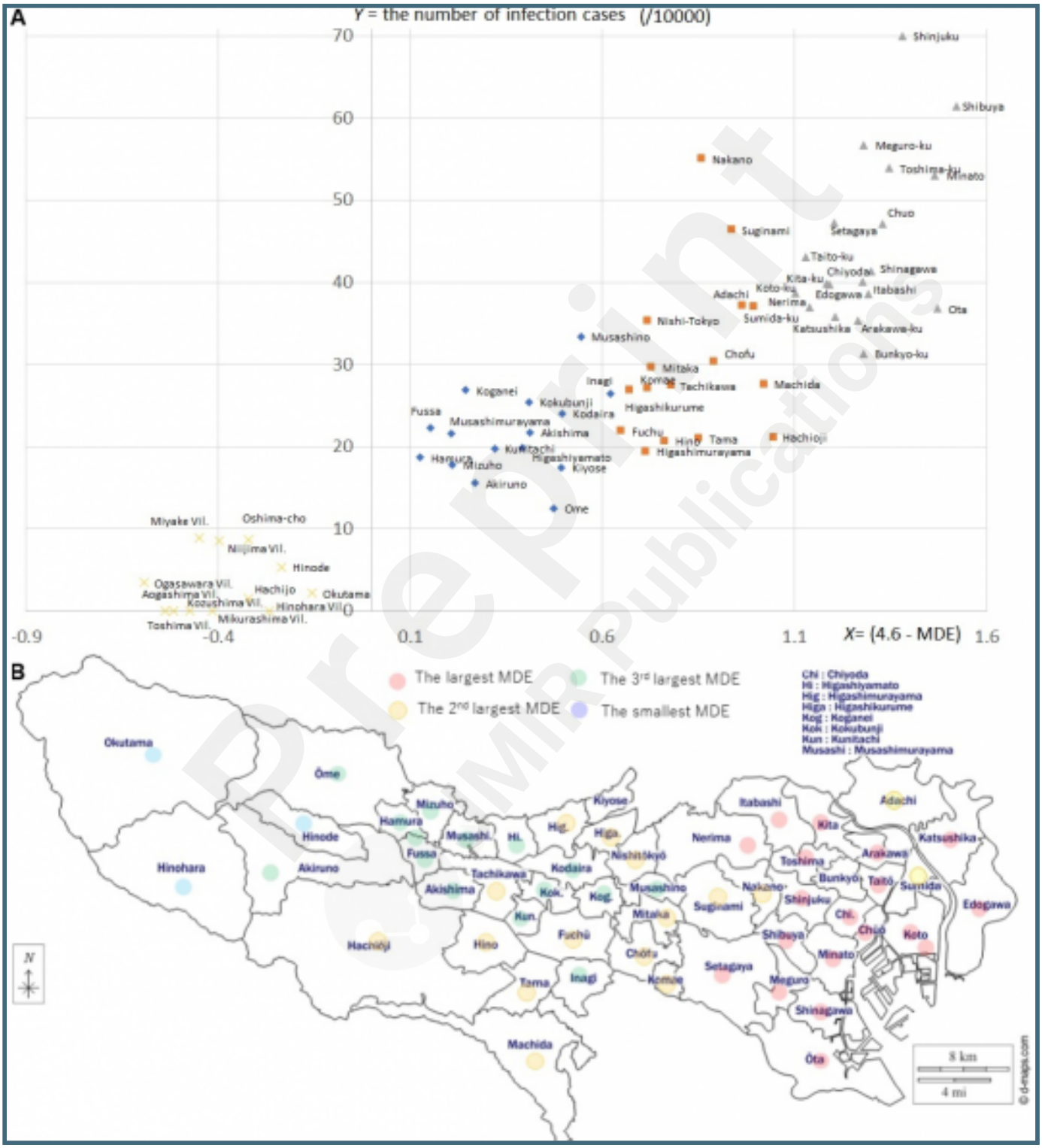

Transition of MDE in local regions classified according to population density (A: permanent, B: daytime, C: influx flow). In B and C, MDE in Class 1 increased during the period of COVID-19 infection expansion. Individuals in cities with high inter-regional activities are believed to stay careful in these periods, avoiding densely populated areas, but their movements were against their careful attitudes, according to the results here. Note: We do not show error bars as of MDE (X-axis) for the reason discussed in “MDE” of Methods.

The maps of 100m meshes in A: all Tokyo except islands and B: a part near the University of Tokyo, with high MDE; stations are classified on the MDE values (red: top 1000 meshes in Tokyo, yellow: the second top 1000 meshes, green: the third, blue: the fourth). All use free-license maps: A: Tokyo free map [46], B: Blank maps from the Geospatial Information Authority of Japan [54].

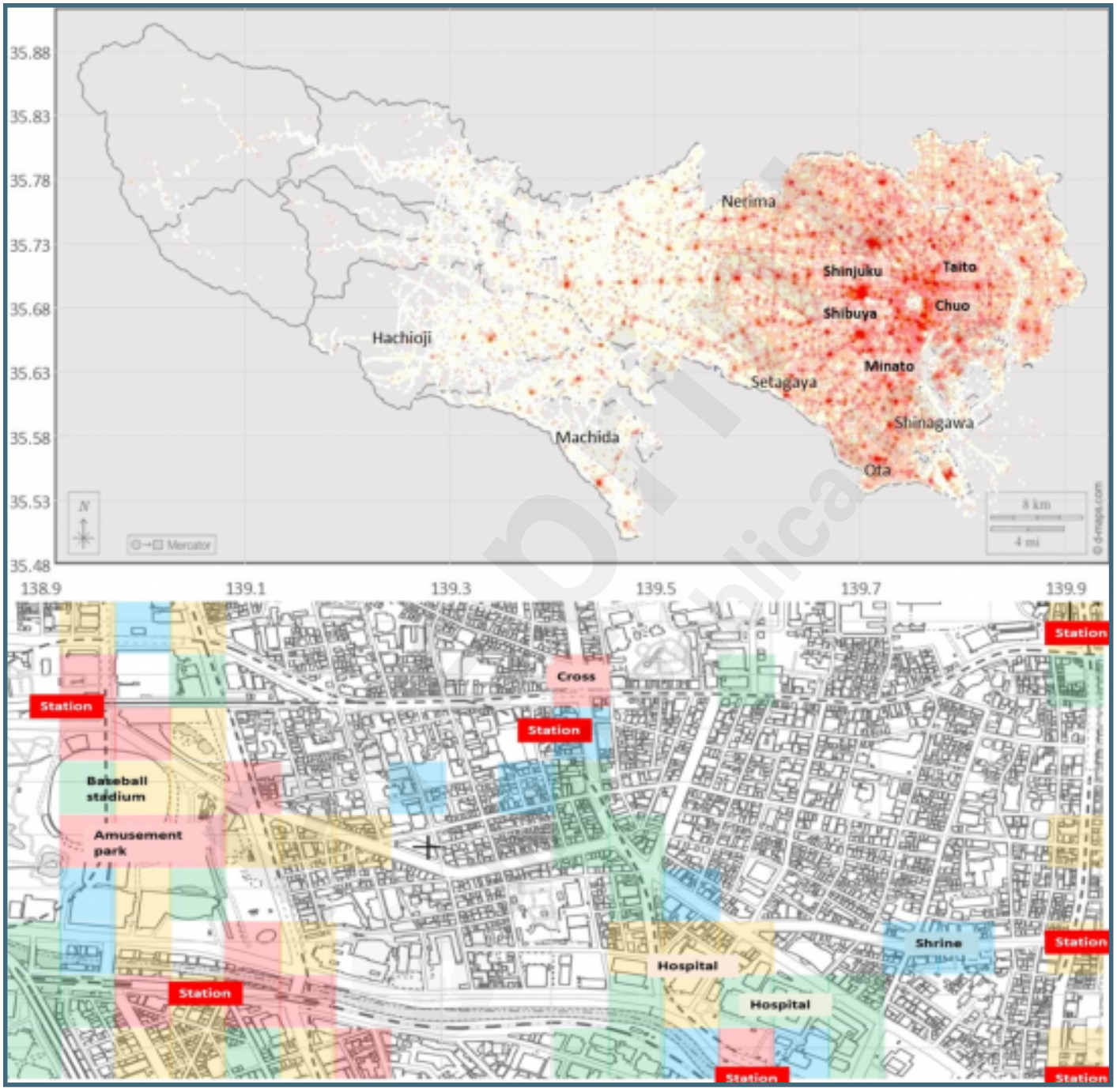

Multimedia Appendixes

Datasets generated or used in this study.
URL: http://asset.jmir.pub/assets/b98f0aa94a69cffd7db422d541fc5a34.docx